Proceedings of the ASME 2016 35th International Conference on Ocean, Offshore and Arctic Engineering
OMAE2016
June 19-24, 2016, Busan, South Korea

OMAE2016-54554

LOCAL STRAIN AND STRESS CALCULATION METHODS OF IRREGULAR HONEYCOMBS UNDER DYNAMIC COMPRESSION

Jilin Yu*
CAS Key Laboratory of Mechanical Behavior and Design of Materials, University of Science and Technology of China
Hefei, Anhui 230026, PR China

Peng Wang
CAS Key Laboratory of Mechanical Behavior and Design of Materials, University of Science and Technology of China
Hefei, Anhui 230026, PR China

Shenfei Liao
National Key Laboratory of Shock Wave and Detonation Physics,
Institute of Fluid Physics, CAEP
Mianyang, Sichuan 621900, PR China

Zhijun Zheng
CAS Key Laboratory of Mechanical Behavior and Design of Materials, University of Science and Technology of China
Hefei, Anhui 230026, PR China

ABSTRACT

Several continuum-based shock models have been proposed to understand the dynamic compressive behavior of cellular materials, but they are mainly based on the quasi-static stress–strain relation and thus lack sufficient dynamic stress–strain information. A virtual 'test' of irregular honeycombs under constant-velocity compression is carried out using the finite element method. A method based on the optimization of local deformation gradient by using the least square method is employed to calculate the one-dimensional strain distribution in the loading direction of the specimen. Meanwhile, a method based on the cross-sectional engineering stress is developed to obtain the one-dimensional stress distribution in the loading direction. The two typical features of cellular materials under dynamic crushing, namely deformation localization and strength enhancement, can be characterized by the strain and stress distributions, respectively. The results also confirm the existence of plastic shock front propagation in cellular structures under high-velocity impact, from which the shock wave speed can be estimated. The shock wave speed obtained from the local strain field method coincides with that from the cross-sectional stress method. The results of shock wave speed are also compared with those predicted by continuum-based shock models. It is shown that the shock wave speed predicted by the R-PP-L (rate-independent, rigid–perfect plastic–locking) shock model or the R-LHP-L (rate-independent, rigid–linearly hardening plastic–locking) shock model is overestimated, but that predicted by the R-PH (rate-independent, rigid–plastic hardening) shock model is close to those obtained from the local strain and cross-sectional stress calculations using the cell-based finite element model.

KEYWORDS

Irregular honeycomb; High-velocity compression; Finite element method; Strain and stress calculation; Shock wave speed.

INTRODUCTION

Cellular materials, such as honeycombs and foams, have gained much research attention due to their excellent mechanical properties in energy absorption and shock mitigation [1]. Many researches have been focused on the two typical features of cellular materials under dynamic crushing, i.e. deformation localization and strength enhancement.

The concept of "structural shock" was proposed by Reid and Peng [2] to describe the localized deformation propagation in wood. Localized deformation was also observed in the dynamic crushing of regular honeycombs by Ruan et al. [3] and irregular honeycombs by Zheng et al. [4] and Liu et al. [5]. Three deformation modes, i.e. Homogeneous mode, Transitional mode and Shock mode, were observed and summarized [4, 5]. Several shock models have been proposed to describe the dynamic behavior of cellular materials, such as the R-PP-L (rigid–perfect plastic–locking) shock model [2], the R-LHP-L (rigid–linearly hardening plastic–locking) shock model [6] and the R-PH (rigid–plastic hardening) shock model [7]. These models are based on one-dimensional continuum

* Corresponding author. E-mail: jlyu@ustc.edu.cn (J.L.Yu)

hypothesis and provide explanation to the enhancement of crushing strength. However, the rationality of the hypothesis is still debatable, see Ref. [8]. Moreover, these models are based on different simplified quasi-static stress-strain curves, lack of direct information of strain and stress in cellular materials.

Herein, a virtual 'test' of Voronoi honeycombs under constant-velocity compression is carried out using the finite element method. A method based on the optimal deformation gradient technique to calculate the local strain field is employed to demonstrate the deformation localization. Furthermore, a method based on the cross-sectional stress is proposed to reveal the strength enhancement. The shock wave speed is then calculated and compared with those predicted by shock models.

NUMERICAL MODEL

The 2D Voronoi technique is employed here to construct irregular honeycombs, see Ref. [4] for details. A sample of Voronoi honeycomb is illustrated in Figure 1, which has 500 cells. The cell irregularity k of the specimen is 0.3 and the relative density ρ_0/ρ_s is 0.1, where ρ_0 is the initial density of Voronoi honeycomb and ρ_s the density of matrix material. The length, width and thickness of the specimen are 50 mm, 50 mm and 1 mm, respectively. The average cell size, which is defined as the diameter of a circle whose area is equal to the average area of Voronoi cells, is about 2.5 mm.

The finite element code ABAQUS/Explicit is employed to perform virtual tests. The specimen shown in Figure 1 is modeled with S4R elements. The material of cell walls is assumed to be elastic, perfectly plastic with Young's modulus E = 66 GPa, Poisson's ratio v = 0.3, yield stress σ_{ys} = 175 MPa, and density ρ_s = 2700 kg/m^3. All nodes are constrained in the out-of-plane direction to simulate a plane strain situation. General contact is applied and the friction coefficient is assumed to be 0.02.

The specimen is placed between two rigid plates: one is fixed and the other moves with a constant velocity V along the X direction, as schematically illustrated in Figure 1.

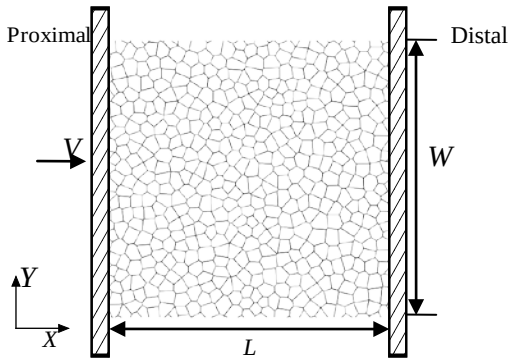

Figure 1. Finite element model of Voronoi structure.

STRAIN FIELD CALCULATION METHOD

In the continuum mechanics, strain tensor is used to describe the level of local deformation. The Lagrangian or Green strain tensor, **E**, is appropriate for the large deformation situation. It is defined as

$$\mathbf{E} = \frac{1}{2}\left(\mathbf{F}^{\mathrm{T}} \cdot \mathbf{F} - \mathbf{I}\right), \tag{1}$$

where **F** is deformation gradient tensor, **I** the identity matrix and superscript T denotes the transpose of a matrix. Thus, a local strain tensor can be obtained when the deformation gradient is determined.

Local strain field calculation method for irregular honeycombs was developed by Liao et al. [9] through the determination of discrete local deformation gradients based on the least square method. A specific deformation gradient **F** cannot accurately map each corner node i together with its neighbor nodes from the reference configuration to the current configuration because of the heterogeneous deformation at the scale of cell. Thus, it is assumed that there exists an optimal local deformation gradient $\mathbf{F}_i$ defined at node i, in a sense of least square approximation, best mapping all the vectors between corner node i and its neighbors from the reference configuration to the current configuration with the smallest error. According to this method, the optimal deformation gradient at the corner node i is formulized as

$$\mathbf{F}_i = \mathbf{W}_i \cdot \mathbf{V}_i^{-1}, \tag{2}$$

where matrix $\mathbf{V}_i$ and $\mathbf{W}_i$ are respectively

$$\begin{cases} \mathbf{V}_i = \sum_{j=1}^{N} \mathbf{U}_{ij} \cdot \mathbf{U}_{ij}^{T} \\ \mathbf{W}_i = \sum_{j=1}^{N} \mathbf{u}_{ij} \cdot \mathbf{U}_{ij}^{T}. \end{cases} \tag{3}$$

In this equation, N is the number of neighboring nodes of node i within a cut-off radius. $\mathbf{U}_{ij}$ and $\mathbf{u}_{ij}$ are the relative position vectors of nodes i and j in the reference and current configurations, respectively.

Combining Eqs (1-3) leads to the determination of local strain tensor **E**. The frequently-used local engineering strain in the Cartesian direction of X_I (I = 1, 2, 3) at a given node is given by

$$\varepsilon_I = 1 - \sqrt{1 + 2E_{II}}. \tag{4}$$

where E_{II} is the diagonal term of **E** in the X_I direction. The strain is taken as positive in compression. The data of 2D discrete strains can be interpolated into a 2D continuous strain field by using Matlab function TriScatteredInterp to treat the Voronoi structure as a 2D continuum. A one-dimensional strain distribution in the loading direction is then obtained by averaging the local engineering strain in the strain field along Y direction.

CONVERGENCE ANALYSIS OF CUT-OFF RADIUS

In the strain calculation method, the local strain of a node is sensitive to the cut-off radius r_c, which determines the number of neighboring nodes around the node. The cut-off radius can be constructed based on the reference configuration or current configuration. In the constant-velocity compression scenario, the nominal strain ε_N is defined as the compression distance divided by the length of the specimen along the loading direction. The mean of all local strains in the specimen, which is defined as

$$\varepsilon_m = \frac{1}{L}\int_0^L \varepsilon_1(X)dX, \tag{5}$$

should be equal to the nominal strain when the local strains are correctly defined and calculated. The relative error of ε_N and ε_m, denoted as δ, is given by $|\varepsilon_N - \varepsilon_m|/\varepsilon_N$. The variations of ε_m and δ with different r_c at nominal strain 0.5 under the velocity of 1 m/s are shown in Figure 2. According to the figure, we can choose R_c/r to be about 1.5 and 0.5 based on the reference and the current configuration, respectively, to control the relative error less than 10%. In this study, the reference and current configurations are both considered with R_c/r being set to be 1.5 and 0.5, respectively.

1D STRESS DISTRIBUTION CALCULATION METHOD

In the cell-based finite element models, micro-structural deformation can be accurately represented. Information such as stress and strain of every element can be obtained from the ABAQUS output file but it is not enough to represent the local stress at the continuum level. In this study, the one-dimensional engineering stress is defined at different Lagrangian locations of cross-sections. At each Lagrangian cross-section, the cross-sectional internal force is composed of two parts of forces. One is caused by the stress in the elements and the other is caused by the cell-wall contact. These two parts of forces, named as nodal force and contact force, can be obtained from the ABAQUS output file, denoted as $\mathbf{F}_N$ and $\mathbf{F}_C$, respectively.

The nodal force and the contact force at the Lagrangian cross-section X can be calculated by

$$\begin{cases} F_{Nx} = \sum_{i=1}^{M} F_{Nxi} \\ F_{Cx} = \sum_{i=1}^{N} \left(F_{CNxi} + F_{CTxi} \right) \end{cases}, \tag{6}$$

where M is the number of the nodes that are at the left side of the elements crossed by the cross-section in the reference configuration, N the number of contact pairs located on the cross-section at the current moment. The variables F_{Nxi}, F_{CNxi} and F_{CTxi} refer respectively to the X-directional components of nodal force, normal contact force and tangential contact force obtained from the ABAQUS output file. Thus, the cross-sectional internal force F_x can be calculated by F_{Nx} plus F_{Cx}.

Based on the continuum hypothesis, the cross-sectional engineering stress is obtained as the force F_x divided by the cross-sectional area of the honeycomb.

(a)

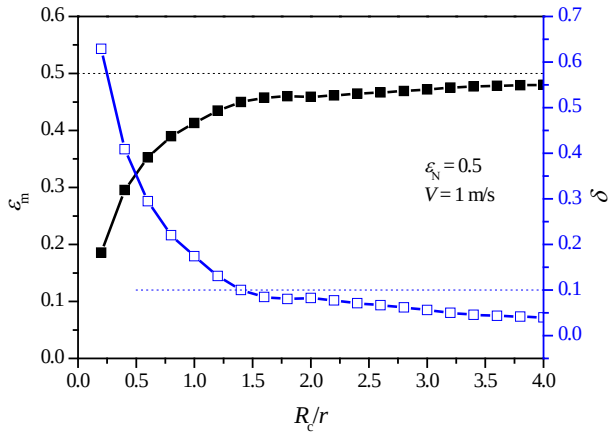

(b)

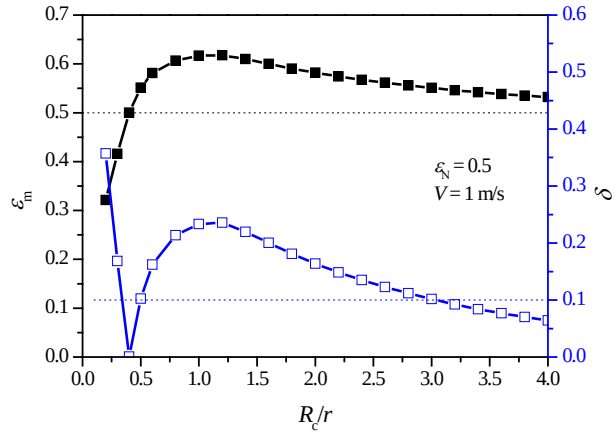

Figure 2. Variations of ε_m and δ with the cut-off radius R_c/r based on (a) the reference configuration and (b) the current configuration.

STRAIN FIELD AND 1D STRESS DISTRIBUTION

The engineering strain fields in the loading direction of the specimens together with the deformation patterns at different nominal strains and different impact velocities are shown in Figure 3. Under a low impact velocity (say 1m/s), random shear collapse bands occur in the specimen due to the randomness and irregularity of cells. The heterogeneous deformation is clearly observed in the engineering strain field corresponding to the deformation pattern, as shown in Figure 3(a). When the

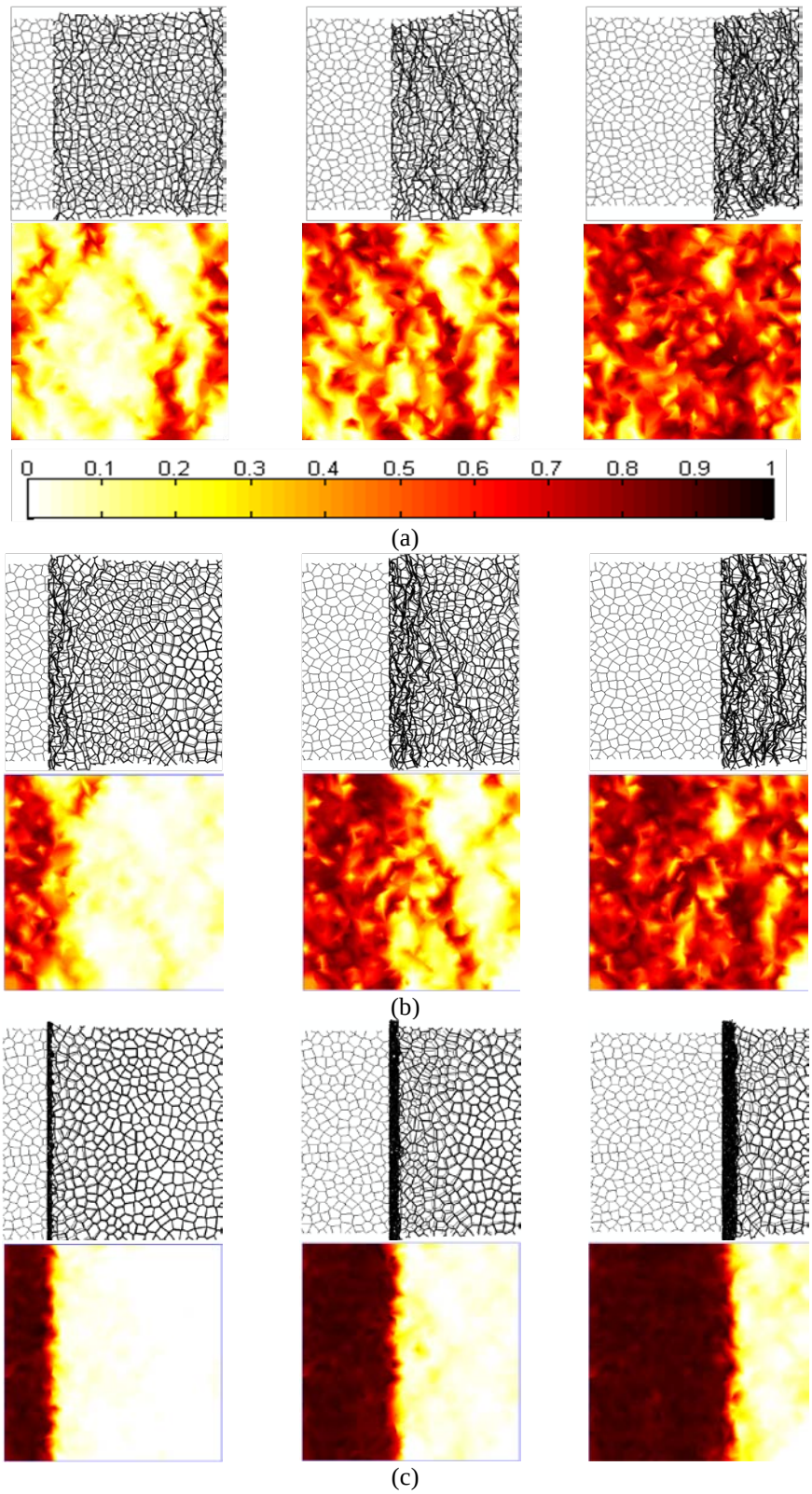

Figure 3. Local engineering strain distributions in the loading direction together with deformation patterns at nominal strains of 0.2, 0.4 and 0.6 under the impact velocities of (a) 1 m/s, (b) 40 m/s and (c) 200 m/s

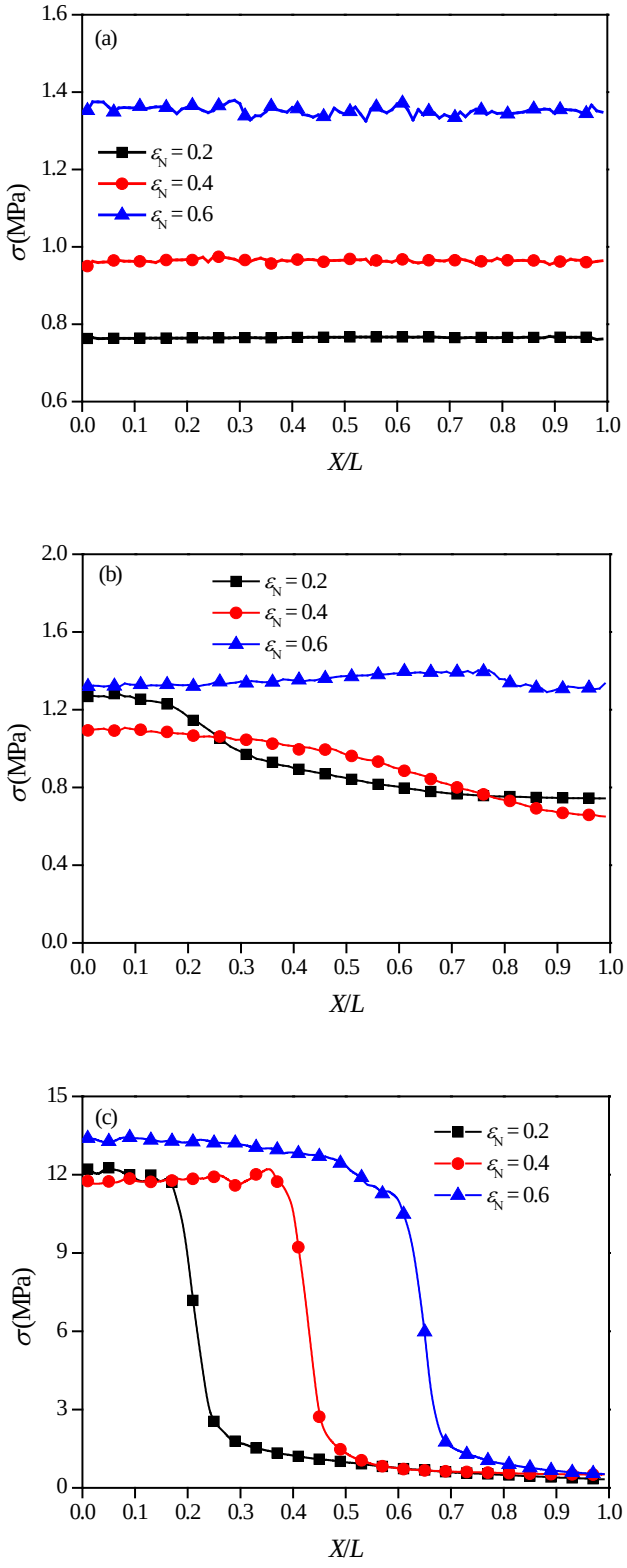

Figure 4. Distributions of stress at different impact velocities. (a) V = 1 m/s, (b) V = 40 m/s and (c) V = 200 m/s.

impact velocity is high enough (say 200 m/s), layer-wise collapse bands are observed. The deformation locates near the proximal end and propagates like a one-dimensional shock wave as the nominal strain increases, as shown in Figure 3(c). Under a moderate impact velocity (say 40 m/s), the characteristic of the shock wave is less obvious than that of 200 m/s, and the strain behind the shock front does not reach the densification strain.

The three deformation modes described above are termed as Homogeneous mode, Transitional mode and Shock mode [4, 5] under low-, moderate- and high-velocity impact, respectively. Distributions of stress at different impact velocities are shown in Figure 4. At the impact velocity of 1 m/s, the stress distribution in the specimen is almost invariable, indicating that the specimen is in a state of force balance, as shown in Figure 4(a). When the deformation mode changes to the Shock mode, a shock-like suddenly change of stress is observed. The stress behind the shock front is obviously higher than that ahead of the shock front, indicating the occurrence of strength enhancement, as shown in Figure 4(c). In the Transitional mode, the stress in the region near the proximal end is higher than that near the support end but less than that in the Shock mode, as shown in Figure 4(b).

SHOCK WAVE SPEED

The phenomenon of shock wave propagation is observed in Figures 3 and 4 for the specimen impacted at V = 200 m/s. The strain gradient and stress gradient are used here to decide the location of the shock front, as shown in Figure 5. Here, the location of the shock front, Φ, is defined as the Lagrangian coordinate X when the absolute strain gradient or stress gradient reaches the maximum value.

The shock wave speed can be obtained from the relation between the Lagrangian locations of the shock front and the impact time, which is shown in Figure 6. Through linear fitting of the data, the shock wave speed can be estimated by the slope of the line.

Comparisons of the shock wave speed predicted by the cross-sectional stress method, the local strain field method and one-dimensional continuum shock models at different impact velocities are shown in Figure 7. It is seen that the shock wave speed predicted by the strain field method almost coincides with that predicted by the cross-sectional stress method, indicating the reliability of the two methods. The shock wave speed predicted by the R-PP-L model or the R-LHP-L model is much higher than those predicted by the strain field method and cross-sectional stress method, especially at very high impact velocities. This is because that the locking strain ε_D used by these two shock models is a velocity- independent constant but in fact the locking strain increases with the impact velocity, as pointed out by Zou et al. [10]. However, the densification strain in the R-PH model depends on the impact velocity and is usually larger than that in the R-PP-L model, leading to a

smaller shock wave speed, which is close to those predicted by the strain field method and cross-sectional stress method.

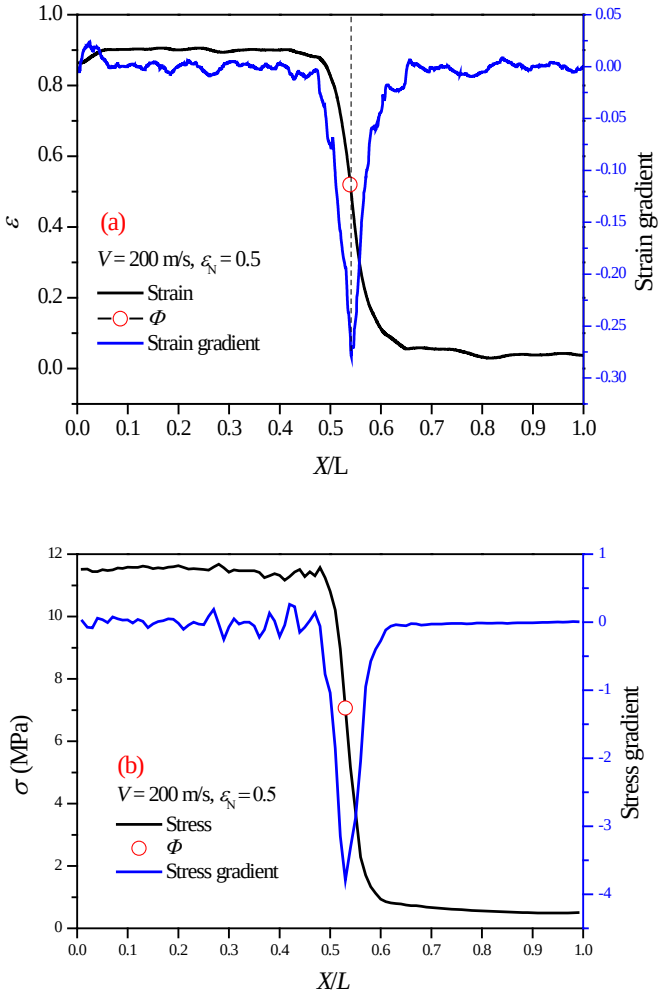

Figure 5. (a) Strain distribution and corresponding strain gradient, and (b) stress distribution and corresponding stress gradient.

CONCLUSIONS

Local strain field and one-dimensional stress distribution are calculated from the results of cell-based finite element simulation of irregular honeycombs under dynamic compression, which clearly show the two typical features of deformation localization and strength enhancement. The existence of shock wave propagation in specimens is confirmed. Comparisons of shock wave speeds predicted by the strain field method, the cross-sectional stress method and one-dimensional shock models are carried out. It is shown that the shock wave speed predicted by the strain field method almost coincides with that predicted by the cross-sectional stress method, indicating the reliability of the two methods. The shock wave speed predicted by R-PH model is close to those predicted by the strain field method and cross-sectional stress method but the shock wave speed predicted by the R-PP-L model or the R-LHP-L model is overestimated.

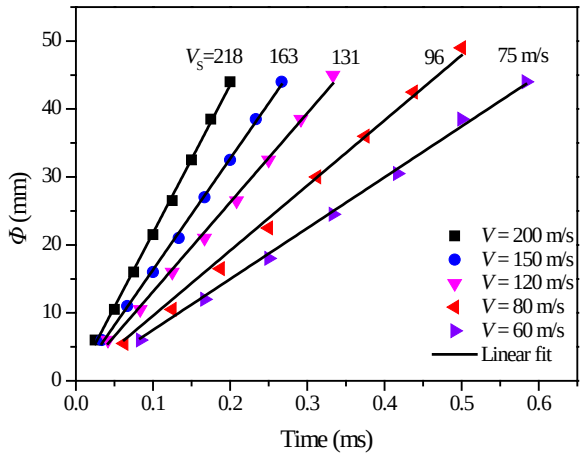

Figure 6. Variations of the Lagrangian locations with time for different impact velocities.

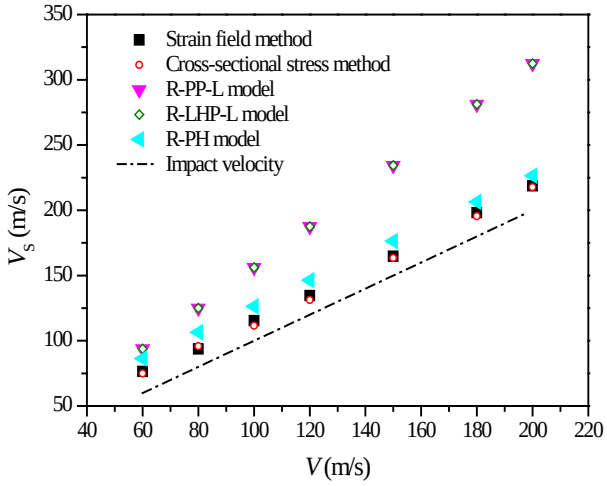

Figure 7. Comparisons of the shock wave speeds among different methods.

ACKNOWLEDGMENTS

This work is supported by the National Natural Science Foundation of China (Project Nos. 11372308 and 11372307) and the Fundamental Research Funds for the Central Universities (Grant No. WK2480000001).

REFERENCES

[1] Lu, G.X., and Yu, T.X., 2003, Energy absorption of

structures and materials, Woodhead Publishing ltd, Cambridge, UK.

[2] Reid, S.R., and Peng, C., 1997, "Dynamic Uniaxial Crushing of Wood," International Journal of Impact Engineering, 19(5-6), pp. 531-570.

[3] Ruan, D., Lu, G.X., Wang, B., and Yu, T.X., 2003, "In-plane Dynamic Crushing of Honeycombs-A Finite Element Study," International Journal of Impact Engineering, 28, pp. 161-182.

[4] Zheng, Z.J., Yu, J.L., and Li, J.R., 2005, "Dynamic Crushing of 2D Cellular Structures: A Finite Element Study," International Journal of Impact Engineering, 32(1-4), pp. 650-664.

[5] Liu, Y.D., Yu, J.L., Zheng, Z.J., and Li, J.R., 2009, "A Numerical Study On the Rate Sensitivity of Cellular Metals," International Journal of Solids and Structures, 46(22-23), pp. 3988-3998.

[6] Zheng, Z.J., Liu, Y.D., Yu, J.L., and Reid, S.R., 2012, "Dynamic Crushing of Cellular Materials: Continuum-based Wave Models for the Transitional and Shock Modes," International Journal of Impact Engineering, 42, pp. 66-79.

[7] Zheng, Z.J., Yu, J.L., Wang, C.F., Liao, S.F., and Liu, Y.D., 2013, "Dynamic Crushing of Cellular Materials: A Unified Framework of Plastic Shock Wave Models," International Journal of Impact Engineering , 53, pp. 29-43.

[8] Harrigan, J.J., Reid, S.R., Tan, P.J., and Reddy, T.Y., 2005, "High Rate Crushing of Wood Along the Grain," International Journal of Mechanical Sciences , 47(4-5), pp. 521-544.

[9] Liao, S.F., Zheng, Z.J., and Yu, J.L., 2013, "Dynamic Crushing of 2D Cellular Structures: Local Strain Field and Shock Wave Velocity," International Journal of Impact Engineering, 57, pp. 7-16.

[10] Zou, Z., Reid, S.R., Tan, P.J., Li, S., and Harrigan, J.J., 2009, "Dynamic Crushing of Honeycombs and Features of Shock Fronts," International Journal of Impact Engineering, 36(1), pp. 165-176.